Quantum speedup dynamics process in multiqubit-interacting system

Ji-Yang Sun, Kai Xu,* and Zai-Dong Li†

Tianjin Key Laboratory of Quantum Optics and Intelligent Photonics, School of Science, Tianjin University of Technology, Tianjin 300384, China

(Received 1 October 2023; accepted 15 February 2024; published 22 March 2024)

We investigate the dynamics of an N-qubit interacting system coupled to a common reservoir. In the weak system-environment coupling regime, the crossovers from Markovian to non-Markovian and from no speedup to speedup can be realized by adjusting the controllable parameters (i.e., the coupling strength between qubits and the number of the qubits). However, in the case of strong coupling, the multiple transitions from non-Markovian regime to Markovian regime and from speedup to no speedup can be induced by manipulating controllable parameters. In addition, a phenomenon can be noticed that the number of qubits and the coupling strength between the qubits have the different effect on the non-Markovian dynamics and speedup evolution of the system in the above weak- and strong-coupling regimes. Our results provide an effective theoretical scheme for the realization of non-Markovian speedup dynamic processes.

DOI: 10.1103/PhysRevResearch.6.013317

I. INTRODUCTION

In most practical situations, a quantum system should be considered an open system [1,2] because it is inevitably coupled to various environments. A simple way to describe the dynamics of open systems is based on Markovian approximation, which is reasonable when the observed evolutionary time scale is much larger than the correlation time of the environment. In this description, the environment is memoryless and can recover instantly from the interaction, which leads to a monotonic one-way flow of information from the system to the environment. Although the Markovian approximation is widely used, the non-Markovian dynamics would emerge [3,4], and backflow of information from the environment to the system occurs when the memory effect of the environment plays a non-negligible role in the dynamics of quantum systems [5–10]. Non-Markovian dynamics not only embody important physical phenomena related to dynamical memory effects, but also prove to be useful in practical processes such as quantum state engineering and quantum control [11–13]. Therefore, more and more researchers begin to pay attention to the conditions under which the non-Markovian dynamic behavior of the system occurs [14–21]. Several mechanisms that trigger non-Markovian dynamics have been discovered, such as structured environments [14–16] and initial system-environment correlations [17–21]. Different methods for quantifying non-Markovian processes or non-Markovianity have been proposed [22–28]. The use of non-Markovianity to protect quantum entanglement and quantum coherence [29–32] has also been widely explored in detail.

Recently, some researchers have studied the effect of non-Markovianity on the speedup of quantum systems [33–43]. In the strong system-environment coupling regime, by considering a qubit in a lossy single-mode cavity, the non-Markovian effects could lead to quantum speedup dynamics [33]. The non-Markovian speedup can also be achieved by controlling the number of the qubits [38]. In some experimental systems, the interaction between qubits exists and plays an important role in the evolution of the system [44–47]. For example, in solid-state nuclear magnetic resonance quantum computing, two-qubit operation requires a switchable interqubit coupling that controls the time evolutions of entanglements [44]. In cavity QED systems, the dipole-dipole interaction cannot be ignored when the distance between qubits is less than the wavelength of the field [45]. In current Rydberg atom experiments, the strong interaction between Rydberg states inhibits multiple excitations within a blockade sphere, and opens the way toward the development of Rydberg quantum simulators [46,47]. Therefore, the effect of the coupling between the qubits on the dynamical evolution of the system should be considered.

Here, we mainly study the dynamics of N interacting qubits coupled with a zero-temperature reservoir. Using quantum speed limit time (QSL time) [48–52] to define the accelerated evolution process, the influence of the coupling strength between qubits and the number of the qubits on the evolution speed of quantum systems is discussed. In the weak coupling between the qubits and a zero-temperature reservoir, the dynamics crossovers from Markovian to non-Markovian and from no speedup to speedup can be achieved by adjusting the coupling strength between qubits. Furthermore, we also analyze the effect of the parameters (i.e., the

*Corresponding author: kxu19930314@163.com
†Corresponding author: lizd@email.tjut.edu.cn

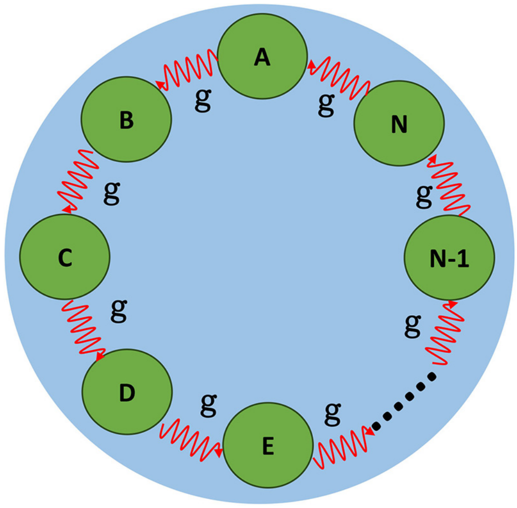

FIG. 1. The figure corresponds to N qubits (green circle) coupled into a common zero-temperature reservoir (blue circle), where each qubit interacts with its two neighbors.

coupling strength between the qubits and the number of the qubits) on the non-Markovian speedup evolution of the qubit in the strong-coupling regime between the qubits and the reservoir.

This paper is organized as follows. In Sec. II, we present a physical model of interacting qubits coupled to a common heat reservoir. In Sec. III, we have provided a useful preliminary to non-Markovianity and then calculated them for the proposed system. In Sec. IV, the effects of the number of qubits and the coupling strength between qubits on the QSL time are discussed. Finally, a simple conclusion of this paper is given in Sec. V.

II. MODELS

We consider N interacting qubits coupled to a common zero-temperature reservoir, as shown in Fig. 1. Here we chose a completely solvable Ising-type coupling model to understand the effects of the qubit-qubit interaction. Each qubit interacts with its neighbors via the Ising-type coupling. The Hamiltonian of the total system can be written as

$$\hat{H} = \hat{H}_S + \hat{H}_R + \hat{H}_{SR}, \tag{1}$$

where

$$\hat{H}_S = \frac{1}{2}\hbar\omega_0 \sum_{j=1}^{N} \hat{\sigma}_j^z + \frac{1}{2}\hbar g \sum_{j=1}^{N} \hat{\sigma}_j^z \hat{\sigma}_{j+1}^z, \tag{2}$$

$$\hat{H}_R = \sum_k \hbar\omega_k \hat{a}_k^\dagger \hat{a}_k, \tag{3}$$

$$\hat{H}_{SR} = \sum_{j=1}^{N} \rho_j \sum_k \hbar(\lambda_k \hat{\sigma}_j^+ \hat{a}_k + \lambda_k^* \hat{\sigma}_j^- \hat{a}_k^\dagger), \tag{4}$$

with the N-qubit Hamiltonian having the periodic boundary condition. In the above expression, $\hat{\sigma}_j^z$ is the Pauli operator of the jth qubit with transition frequency ω_0, $\hat{\sigma}_j^+$ ($\hat{\sigma}_j^-$) the raising (lowering) operator of the jth qubit, $\hat{a}_k$ and $\hat{a}_k^\dagger$ are the lowering and raising operators of the kth oscillator of the zero-temperature reservoirs with frequency ω_k, and the constant parameter g represents the strength of the qubit-qubit interaction. The constant factor ρ_j is introduced in Eq. (4) to distinguish qubits. Therefore, the actual coupling strength between the jth qubit and the kth field mode is given by $\rho_j|\lambda_k|$ [53,54].

Then, for convenience, we solve the dynamical evolution process of the system in the interaction picture. The Hamiltonian of the total system in the interaction picture can be expressed as

$$\hat{H}_{SR}(t) = \hbar \sum_{j=1}^{N} \sum_k \rho_j [\lambda_k \hat{\sigma}_j^+ \hat{a}_k e^{-i\varphi} + \lambda_k^* \hat{\sigma}_j^- \hat{a}_k^\dagger e^{i\varphi}], \tag{5}$$

where $\varphi(t) \equiv [\omega_k - \omega_0 - g(\hat{\sigma}_{j+1}^z + \hat{\sigma}_{j-1}^z)]t$. To solve the Schrodinger equation, we first assume that the initial state of the total system is $|\psi(0)\rangle = |g\rangle_{1st=e}^{\otimes N} \otimes |\mathbf{0}\rangle$, where $|g\rangle_{1th=e}^{\otimes N}$ means that the first qubit is in the excited state and the remaining $N-1$ qubits are in the ground state, and $|\mathbf{0}\rangle$ means that the reservoir is in the vacuum state. After time $t > 0$, the state of the total system evolves to the following one: $|\psi(t)\rangle = [\alpha_1(t)|g\rangle_{1st=e}^{\otimes N} + \alpha_2(t)|g\rangle_{2nd=e}^{\otimes N} + \cdots + \alpha_N(t)|g\rangle_{Nth=e}^{\otimes N}] \otimes |\mathbf{0}\rangle + |g\rangle^{\otimes N} \otimes \sum_k \beta_k(t)|\mathbf{1_k}\rangle$, where $|\mathbf{1_k}\rangle = |0...1_k...0\rangle$ means that the kth harmonic oscillator of the reservoir is in the excited state. Therefore, theses amplitudes $\alpha_1(t)$, $\alpha_2(t)$,..., $\alpha_N(t)$ are given by the following integrodifferential equation:

$$\frac{d\alpha_j}{dt} = -\rho_j \sum_{j=1}^{N} \int_0^t f(t-t^{'}) e^{-2ig(t-t^{'})} \rho_j \alpha_j(t^{'}) dt^{'}, \tag{6}$$

where the correlation function $f(t-t') = \int d\omega J(\omega) e^{-i(\omega_k-\omega_0)(t-t')}$ is related to the spectral density $J(\omega)$ of the reservoir. The reservoir is assumed as a Lorentzian spectral density, i.e., $J(\omega) = \gamma_0\lambda^2/(2\pi(\omega-\omega_0)^2 + \lambda^2)$, where γ_0 is the system-reservoir coupling strength, and λ^{-1} is the reservoir correlation time. It is well known that the standard Laplace transform technique is an effective method to get the solution of Eq. (6). Here we focus on the dynamics behavior of the first qubit. The reduced density matrix of the system is referenced in Appendix A. The probability amplitude $\alpha_1(t)$ can be expressed as $\alpha_1(t) = 1 - 1/N + e^{-(\lambda/2+ig)t}/N \times [\cosh(\Omega t/2) + ((\lambda + 2ig)/\Omega)\sinh(\Omega t/2)]$, where $\Omega = \sqrt{(\lambda + 2ig)^2 - 2\gamma_0\lambda N\rho_j^2}$. From the expression of $\alpha_1(t)$, we want to stress that the dynamical behavior of the system can be modified by the number N of qubits and the coupling strength g between the qubits in the weak ($\lambda > 2\gamma_0$)/strong ($\lambda < 2\gamma_0$) system-environment coupling regime.

III. THE CONTROL OF NON-MARKOVIAN DYNAMICS

To further illustrate the roles of the number N of qubits and the coupling strength g between the qubits, in what follows we describe how to tune the environment from Markovian to non-Markovian by manipulating N and g. To quantify the non-Markovianity, we use the Breuer-Laine-Piilo (BLP) measure which is based on the distinction of trace distances between the dynamics of two

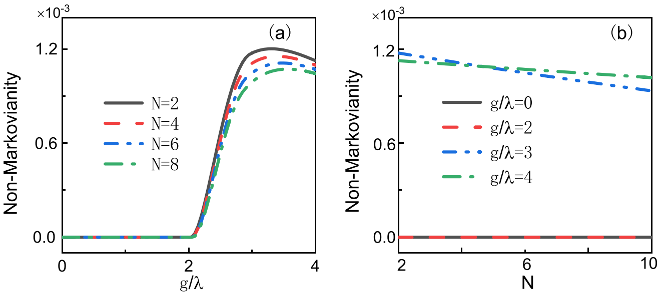

FIG. 2. (a), (b) The non-Markovianity of the quantum system dynamic with $\gamma_0 = 0.1\lambda$ and $\tau = 1$ as a function of the coupling strength g and the number of qubits N in the weak qubit-reservoir coupling regime.

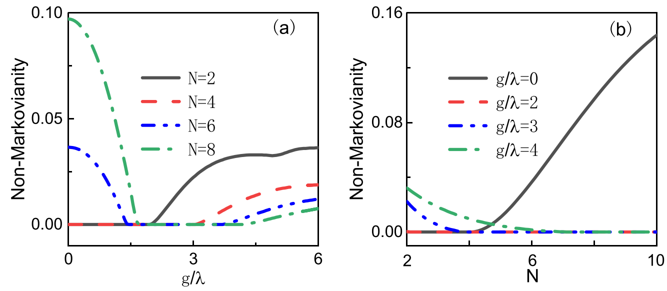

FIG. 3. (a), (b) The non-Markovianity of the quantum system dynamic with $\gamma_0 = 5\lambda$ and $\tau = 1$ as a function of the coupling strength g and the number of qubits N in the strong qubit-reservoir coupling regime.

different initial states of an open system [22]. A Markovian dynamics process of the system cannot improve their trace distance for two different initial states $\rho_1(0)$ and $\rho_2(0)$ of a system, therefore, the growth of the trace distance implies the appearance of non-Markovian dynamics. Based on this concept, the BLP measure of non-Markovianity is given as $\mathcal{N} = \max_{\rho_1(0),\rho_2(0)} \int_{\sigma>0} dt\sigma[t, \rho_1(0), \rho_2(0)]$, with $\sigma[t, \rho_1(0), \rho_2(0)] = d\zeta(\rho_1(t), \rho_2(t))/dt$ [22]. The trace distance $\zeta(\rho_1(t), \rho_2(t))$ is defined as $\zeta(\rho_1(t), \rho_2(t)) = \frac{1}{2}Tr\|\rho_1(t) - \rho_2(t)\|$, where $\|A\| = \sqrt{A^\dagger A}$. To evaluate the non-Markovianity $\mathcal{N}$, one should optimize the initial state of the system. Fortunately, based on the result of Ref. [55] and through numerical calculations, the the optimal initial states of the system maximizing the time derivative of the trace distance can be chosen as $\{|g\rangle, |e\rangle\}$. This allows us to get the rate of change of the trace distance in the simple form $\sigma[t, \rho_1(0), \rho_2(0)] = d|\alpha_1(t)|^2/dt$.

When there are no other qubits, the system's dynamics mainly depends on the parameters λ and γ_0 in such a way that $\lambda > 2\gamma_0$ ($\lambda < 2\gamma_0$), which is identified as the weak-coupling (strong-coupling) regime, leads to Markovian (non-Markovian) dynamics. In the case of adding qubits, the dynamics of the system would be considered in the weak qubit-reservoir coupling regime. In the following, we will discuss the non-Markovianity of system dynamics as the function of the qubit-qubit interaction g and the total numbers of qubits N.

First, we consider the case of weak the qubit-reservoir coupling regime. When the qubit-qubit interaction g is small, the system exhibits Markovian dynamics. However, when the qubit-qubit interaction g exceeds a certain threshold, it has significant non-Markovian dynamics, as shown in Fig. 2(a). It implies that the qubit-qubit coupling play effective roles to trigger the non-Markovian dynamics of the system. We also find that the larger g and the smaller N have more advantage to trigger the stronger non-Markovianity. Then the effect of the number N of qubits on non-Markovianity is shown in Fig. 2(b). It is clear that increasing the number of qubits is not beneficial for improving non-Markovianity. Therefore, in the weak qubit-reservoir coupling regime, the larger g/λ and the smaller N can be required to trigger the stronger non-Markovianity.

When considering the strong coupling of the qubit with the reservoir, the influence of N and g/λ on non-Markovianity is shown in Fig. 3. In Fig. 3(a), for a smaller N (i.e., $N = 2, 4$), a remarkable dynamical crossover from Markovian behavior to non-Markovian behavior can occur at a critical coupling strength g_{cr}/λ. When $g/\lambda < g_{cr}/\lambda$, the dynamics maintains Markovian behavior, and then the non-Markovianity increases monotonically with increasing g/λ. However, for a relatively large N (i.e., $N = 6, 8$), increasing g/λ from zero, the non-Markovianity first diminishes to zero and then rises. This implies that the qubit-qubit coupling is able not only to enhance the non-Markovianity of the environment but also to restrain it. Then the influence of N on the non-Markovianity is shown in Fig. 3(b). When there is a lack of coupling between qubits (i.e., $g/\lambda = 0$), the increase of N promotes the non-Markovianity. While there is a fixed coupling strength between qubits, the increase of N will inhibit the non-Markovianity. Furthermore, it is worth noting that the non-Markovianity of the system dynamics process with $g/\lambda = 0$ and large N is always larger than the non-Markovianity with $g/\lambda > 0$. That is to say, in the strong qubit-reservoir coupling regime, the goal of a strong non-Markovianity require the smaller qubit-qubit interaction g and a larger total numbers of qubits N.

IV. QUANTUM SPEEDUP OF THE SYSTEM DYNAMICS

In order to analyze the role of the number of the qubits and the coupling strength between the qubits on the maximum evolution speed of an open system, we use the definition of quantum speed limit time (QSL time). It can characterize the minimum time required for a quantum system to evolve from the initial state to the target state and can be helpful to analyze the maximal evolution speed of an open quantum system. The QSL time from the initial state $\rho(0) = |\Psi_0\rangle\langle\Psi_0|$ to the target state $\rho(\tau)$ (the evolutional state of the system at the actual evolution time τ) is defined as $\tau_{\mathrm{QSL}} = \sin^2\{\mathbf{B}[\rho(0), \rho(\tau)]\}/\Lambda_\tau^\infty$ [33], where $\mathbf{B}[\rho(0), \rho(\tau)] = \arccos\sqrt{\langle\phi_0|\rho(\tau)|\phi_0\rangle}$ is the Bures angle between initial pure state and its evolved state, and $\Lambda_\tau^\infty = \tau^{-1}\int_0^\tau \|\dot{\rho}(t)\|_\infty dt$ with the operator norm $\|\dot{\rho}(t)\|_\infty$ equaling the largest singular value of $\dot{\rho}(t)$. The tightness of the chosen QSL bound is good (see Appendix C for details). Then for a given evolutionary time, the ratio between the QSL time and the actual evolution time provides an estimate of the potential ability to accelerate the evolution of quantum dynamics. When $\tau_{QSL}/\tau = 1$, there is no further

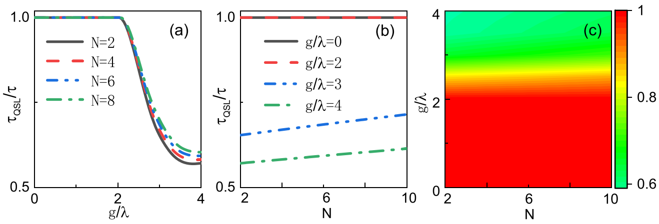

FIG. 4. (a), (b) The τ_{QSL}/τ for the quantum system dynamics with $\gamma_0 = 0.1\lambda$ and $\tau = 1$ in the weak system-environment coupling regime as a function of the coupling strength g and the number of qubits N in a common zero-temperature reservoir. (c) Phase diagram of τ_{QSL}/τ in the g/λ-N-τ_{QSL}/τ plane with $\gamma_0 = 0.1\lambda$ and $\tau = 1$ in the weak qubit-reservoir coupling regime.

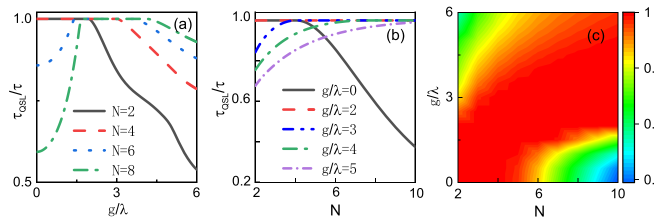

FIG. 5. (a), (b) The τ_{QSL}/τ for the quantum system dynamics with $\gamma_0 = 5\lambda$, and $\tau = 1$ in the strong system-environment coupling regime as a function of the coupling strength g and the number of qubits N in a common zero-temperature reservoir. (c) Phase diagram of τ_{QSL}/τ in the g/λ-N-τ_{QSL}/τ plane with $\gamma_0 = 5\lambda$, and $\tau = 1$ in the strong qubit-reservoir coupling regime.

potential acceleration capability. While $\tau_{QSL}/\tau < 1$, the smaller the ratio, the greater the rate of system evolution.

Then, according to the reduced density matrix of the system and the expression of the QSL time, the QSL time can be simplified as [56]

$$\tau_{QSL} = \frac{1 - |\alpha_1(\tau)|^2}{\frac{1}{\tau}\int_0^\tau |\partial_t|\alpha_1(t)|^2|dt} = \frac{\tau(1 - |\alpha_1(\tau)|^2)}{2\mathcal{N}+1 - |\alpha_1(\tau)|^2}; \quad (7)$$

Eq. (7) shows that the QSL time is equal to the actual evolution time when $\mathcal{N} = 0$, but the QSL time is smaller than the actual evolution time when $\mathcal{N} > 0$. That is, the larger non-Markovianity $\mathcal{N}$ can lead to the faster quantum evolution and the lower QSL time. It is worth mentioning that the relationship between $\mathcal{N}$ and QSL does not depend on whether the non-Markovianity measure is a BLP measure or the coherence-based measure of the non-Markovianity. For a specific process, refer to Appendix B. In what follows, we use Eq. (7) to evaluate the effects of the number N of qubits and the coupling strength g between the qubits on the dynamical evolution speed of the system.

For the weak qubit-reservoir coupling regime, the τ_{QSL}/τ as a function of the controllable parameters (g, N) has been plotted in Fig. 4. From Fig. 4(a) we find that a significant decrease in τ_{QSL}/τ occurs when the qubit-qubit interaction g exceeds a certain critical coupling strength g_{cr}. This implies that the quantum speedup evolution can be realized by manipulating the coupling strength between the qubits. At the same time, when $g > g_{cr}$ we observe that the τ_{QSL}/τ increases with the increasing number of qubits. It implies the acceleration capacity of the system is strong in small numbers of qubits. As for Fig. 4(b), the effect of the number of qubits N on τ_{QSL}/τ is plotted. It is worth noting that, the no-speedup evolution ($\tau_{QSL}/\tau = 1$) could be followed, and the speedup evolution ($\tau_{QSL}/\tau < 1$) would occur when the coupling strength $g > g_c$ between the qubits. And it is clear that the potential acceleration capacity of the system decreases as the number of qubits increases. The detail phase diagram is given in Fig. 4(c) for the τ_{QSL}/τ depending on the the qubits number N and the coupling strength g between the qubits. It conforms that the smaller N and larger g/λ lead to the smaller τ_{QSL}/τ. Therefore, to speed up the quantum system evolution, a larger coupling strength g and a smaller number of the qubits N are required for the weak qubit-environment coupling regime.

In the presence of the strong qubit-reservoir coupling regime, i.e., $\lambda < 2\gamma_0$, the situation is different. To illustrate this difference, we present in Fig. 5 the effects of the coupling strength g/λ between the qubits and the number of qubits N on the τ_{QSL}/τ. Figure 5(a) shows the dependence of τ_{QSL}/τ on g/λ for different N. For relatively small values of N (i.e., $N = 2, 4$), the increase of g/λ can take the dynamical evolution process of the system transition from no-speedup to speedup evolution. For larger values of N, the evolution speed will go from speed down to no speedup and then to speedup evolution by increasing g/λ. This implies that, in the strong qubit-reservoir coupling regime, the speed of evolution for the system can be controlled to a speedup or speed-down process by selecting the appropriate parameters g/λ and N. As for Fig. 5(b), when the coupling between the qubits does not exist (i.e., $g/\lambda = 0$), the increase in the number of qubits can promote the transition of the system from no-speedup evolution to speedup evolution. However, considering $g/\lambda = 2, 3, 4, 5$, the system does not appear to speedup evolution by manipulating N. That is to say, N and g/λ have different effects on the accelerated evolution of the system. A comprehensive picture for the dependence of τ_{QSL}/τ on g/λ and N is shown in Fig. 5(c), where we can see the speedup evolution thresholds of g/λ for a given N and the crossovers between no-speedup and speedup regimes as N increases for a given g/λ. Clearly, in the strong qubit-reservoir coupling regime, to achieve speedup evolution of the system, either the larger N and the smaller g/λ, or the smaller N and the larger g/λ should be chosen.

V. CONCLUSION

In this work, we investigated the dynamics of an N-qubit system immersed in a common zero-temperature reservoir. We showed that two dynamical crossovers of the quantum system, from Markovian to non-Markovian dynamics and from no-speedup evolution to speedup evolution, have been achieved in the weak qubit-reservoir coupling regime by controlling the number N of qubits and the coupling strength g between the qubits. It is worth noting that the coupling strength g and the number N of the qubit have the opposite effect on the non-Markovian dynamics and speedup evolution of the qubit in the weak qubit-reservoir coupling regime. Then, by considering the strong qubit-reservoir coupling regime, manipulation the coupling strength between the qubits and the number of the qubits would take the system multiple crossovers from non-Markovian to Markovian regimes and from speedup to no-speedup regimes. Here, it should be pointed out that, for the systems we consider in the amplitude damping channel, QSL and non-Markovianity can be connected. However, it is worth emphasizing that the connection between QSL and non-Markovianity depends on the dynamical evolution process of the system, so there is no universal connection between QSL and non-Markovianity [57,58].

In addition, our setup is an interacting two-level system that is influenced by the environment. It can be realized by ultracold atoms held by optical lattice [59,60] and by transmon qubits in a circuit QED system [61,62]. In a superconducting circuit system, the interaction between qubits can be regulated by capacitance. Therefore, according to these potential candidates for the qubits, our proposed scheme is experimentally feasible. Our work emphasizes that in multiqubit systems, the non-Markovian speedup dynamical behavior of the system can be realized by manipulating the coupling between the systems.

ACKNOWLEDGMENTS

This work was supported by the National Natural Science Foundation of China Grants No. 12204348 and No. 61774001, and the Program of State Key Laboratory of Quantum Optics and Quantum Optics Devices, Shanxi University, China (Grant No. KF202203).

APPENDIX A: THE REDUCED DENSITY OF THE SINGLE-QUBIT SYSTEM

In this Appendix, we will provide further details on the reduced density matrix discussed in the main text. The density matrix of the whole system can be expressed as

$$\rho^{QS} = |\psi(t)\rangle\langle\psi(t)|, \tag{A1}$$

where

$$|\psi(t)\rangle = \left[\alpha_1(t)|g\rangle^{\otimes N}_{1st=e} + \alpha_2(t)|g\rangle^{\otimes N}_{2nd=e} + \cdots + \alpha_N(t)|g\rangle^{\otimes N}_{Nth=e}\right] \otimes |\mathbf{0}\rangle + |g\rangle^{\otimes N} \otimes \sum_k \beta_k(t)|\mathbf{1_k}\rangle. \tag{A2}$$

Then

$$\begin{aligned}\rho^{QS} &= |\psi(t)\rangle\langle\psi(t)| \\ &= \left\{\left[\alpha_1(t)|g\rangle^{\otimes N}_{1st=e} + \alpha_2(t)|g\rangle^{\otimes N}_{2nd=e} + \cdots + \alpha_N(t)|g\rangle^{\otimes N}_{Nth=e}\right] \otimes |\mathbf{0}\rangle + |g\rangle^{\otimes N} \otimes \sum_k \beta_k(t)|\mathbf{1_k}\rangle\right\} \\ &\quad \times \left\{\left[\alpha_1^*(t)\langle g|^{\otimes N}_{1st=e} + \alpha_2^*(t)\langle g|^{\otimes N}_{2nd=e} + \cdots + \alpha_N^*(t)\langle g|^{\otimes N}_{Nth=e}\right] \otimes \langle\mathbf{0}| + \langle g|^{\otimes N} \otimes \sum_k \beta_k^*(t)\langle\mathbf{1_k}|\right\}.\end{aligned} \tag{A3}$$

After tracing out the zero-temperature thermal reservoir, the reduced density matrix ρ^Q of the N-qubit system is given by

$$\rho^Q = \langle\mathbf{0}|\psi(t)\rangle\langle\psi(t)|\mathbf{0}\rangle + \langle\mathbf{1_k}|\psi(t)\rangle\langle\psi(t)|\mathbf{1_k}\rangle, \tag{A4}$$

where $|\mathbf{0}\rangle = |g, g, g, \ldots, g\rangle$, $|\mathbf{1_k}\rangle = |g, g, g, \ldots, e, \ldots, g\rangle$. We can obtain

$$\begin{aligned}&\langle\mathbf{0}|\psi(t)\rangle\langle\psi(t)|\mathbf{0}\rangle \\ &= \langle\mathbf{0}|\left\{\left[\alpha_1(t)|g\rangle^{\otimes N}_{1st=e} + \alpha_2(t)|g\rangle^{\otimes N}_{2nd=e} + \cdots + \alpha_N(t)|g\rangle^{\otimes N}_{Nth=e}\right] \otimes |\mathbf{0}\rangle + |g\rangle^{\otimes N} \otimes \sum_k \beta_k(t)|\mathbf{1_k}\rangle\right\} \\ &\quad \times \left\{\left[\alpha_1^*(t)\langle g|^{\otimes N}_{1st=e} + \alpha_2^*(t)\langle g|^{\otimes N}_{2nd=e} + \cdots + \alpha_N^*(t)\langle g|^{\otimes N}_{Nth=e}\right] \otimes \langle\mathbf{0}| + \langle g|^{\otimes N} \otimes \sum_k \beta_k^*(t)\langle\mathbf{1_k}|\right\}|\mathbf{0}\rangle \\ &= \left[\alpha_1(t)|g\rangle^{\otimes N}_{1st=e} + \alpha_2(t)|g\rangle^{\otimes N}_{2nd=e} + \cdots + \alpha_N(t)|g\rangle^{\otimes N}_{Nth=e}\right]\left[\alpha_1^*(t)\langle g|^{\otimes N}_{1st=e} + \alpha_2^*(t)\langle g|^{\otimes N}_{2nd=e} + \cdots + \alpha_N^*(t)\langle g|^{\otimes N}_{Nth=e}\right] \\ &= |\alpha_1(t)|^2|g\rangle^{\otimes N}_{1st=e}\langle g|^{\otimes N}_{1st=e} + \alpha_1(t)\alpha_2^*(t)|g\rangle^{\otimes N}_{1st=e}\langle g|^{\otimes N}_{2nd=e} + \cdots + \alpha_1(t)\alpha_N^*(t)|g\rangle^{\otimes N}_{1st=e}\langle g|^{\otimes N}_{Nth=e} \\ &\quad + \alpha_2(t)\alpha_1^*(t)|g\rangle^{\otimes N}_{2nd=e}\langle g|^{\otimes N}_{1st=e} + |\alpha_2(t)|^2|g\rangle^{\otimes N}_{2nd=e}\langle g|^{\otimes N}_{2nd=e} + \cdots + \alpha_2(t)\alpha_N^*(t)|g\rangle^{\otimes N}_{2nd=e}\langle g|^{\otimes N}_{Nth=e} + \cdots \\ &\quad + \alpha_N(t)\alpha_1^*(t)|g\rangle^{\otimes N}_{Nth=e}\langle g|^{\otimes N}_{1st=e} + \alpha_N(t)\alpha_2^*(t)|g\rangle^{\otimes N}_{Nth=e}\langle g|^{\otimes N}_{2nd=e} + \cdots + |\alpha_N(t)|^2|g\rangle^{\otimes N}_{Nth=e}\langle g|^{\otimes N}_{Nth=e}\end{aligned} \tag{A5}$$

$$\begin{aligned}&\langle\mathbf{1_k}|\psi(t)\rangle\langle\psi(t)|\mathbf{1_k}\rangle \\ &= \langle\mathbf{1_k}|\left\{\left[\alpha_1(t)|g\rangle^{\otimes N}_{1st=e} + \alpha_2(t)|g\rangle^{\otimes N}_{2nd=e} + \cdots + \alpha_N(t)|g\rangle^{\otimes N}_{Nth=e}\right] \otimes |\mathbf{0}\rangle + |g\rangle^{\otimes N} \otimes \sum_k \beta_k(t)|\mathbf{1_k}\rangle\right\}\end{aligned}$$

$$\times\left\{\left[\alpha_1^*(t)\langle g|_{1st=e}^{\otimes N}+\alpha_2^*(t)\langle g|_{2nd=e}^{\otimes N}+\cdots+\alpha_N^*(t)\langle g|_{Nth=e}^{\otimes N}\right]\otimes\langle\mathbf{0}|+\langle g|^{\otimes N}\otimes\sum_k\beta_k^*(t)\langle\mathbf{1_k}|\right\}|\mathbf{1_k}\rangle$$
$$=\sum_k|\beta_k(t)|^2|g\rangle^{\otimes N}\langle g|^{\otimes N};\tag{A6}$$

We now consider the speedup dynamics of a single qubit (say the first qubit) in the presence of the other $N-1$ interacting qubits. After tracing out the other qubits, the reduced density matrix ρ of the single-qubit system is given by

$$\rho=\begin{pmatrix}1-|\alpha_1(t)|^2 & 0\\ 0 & |\alpha_1(t)|^2\end{pmatrix},\tag{A7}$$

with the standard base $\{|g\rangle, |e\rangle\}$.

APPENDIX B: THE COHERENCE-BASED MEASURE OF NON-MARKOVIANITY

In this Appendix, we present the coherence-based measure of non-Markovianity, complementing the results shown in the main text. To examine the correlation between the coherence-based measure of non-Markovianity (CMON) and QSL, we first have to give an expression for CMON for the physical model we consider. In Ref. [63], CMON can be written as

$$\mathcal{N}_{\rm CMON}=\max_{\rho(0)\in\{|\Psi_d\rangle\}}\int_{\frac{dC(\rho(t))}{dt}>0}\frac{dC(\rho(t))}{dt}dt,\tag{B1}$$

where $|\Psi_d\rangle=(1/\sqrt{d})\sum_{i=1}^{d}=e^{i\phi_i}|i\rangle$ (d is the dimension of the Hilbert space and $\phi_i\in[0,2\pi)$) and $C(\rho(t))$ is the quantum coherence of the system. In this paper, we consider the system in a dissipative channel. For an arbitrary system qubit [$\rho(0)$], dynamical map $\rho(t)=\Lambda(t)\rho(0)$ is given by [1,64]

$$\rho(t)=\begin{pmatrix}\rho_{00}(0)+\rho_{11}(0)(1-|\alpha_1(t)|^2) & \rho_{01}(0)\alpha_1^*(t)\\ \rho_{10}(0)\alpha_1(t) & \rho_{11}(0)|\alpha_1(t)|^2\end{pmatrix}.\tag{B2}$$

Therefore, the l_1 norm of coherence $C_{l_1}(\rho(t))=2|\rho_{10}(0)||\alpha_1(t)|$, and clearly $d|\alpha_1(t)|/dt>0$ will mark the emergence of non-Markovianity. CMON will simply be

$$\mathcal{N}_{\rm CMON}=\int_{\frac{d|\alpha_1(t)|}{dt}>0}\frac{d|\alpha_1(t)|}{dt}dt.\tag{B3}$$

In our paper, we use the BLP measure to evaluate the non-Markovianity of the environment. The BLP measure of non-Markovianity [22] is given as

$$\mathcal{N}_{\rm BLP}=\max_{\rho_1(0),\rho_2(0)}\int_{\sigma>0}dt\sigma[t,\rho_1(0),\rho_2(0)].\tag{B4}$$

In [56], for the map of equation

$$\Phi_t^{JC}(\rho_0)=\rho(t)=\begin{pmatrix}\rho_{11}|b_t|^2 & \rho_{10}(0)b_t\\ \rho_{01}(0)b_t^* & 1-\rho_{11}|b_t|^2\end{pmatrix},\tag{B5}$$

it was numerically shown that the eigenstates $|0\rangle\langle 0|$ and $|1\rangle\langle 1|$ of σ_3 are the optimal pair of states for the BLP measure. Based on these, the BLP measure of non-Markovianity for our considered model can be written as $\mathcal{N}_{\rm BLP}=\int_{d|\alpha_1(t)|^2/dt>0}(d|\alpha_1(t)|^2/dt)dt$. Comparing the CMON and BLP measures, we can get two points: (i) The conditions for non-Markovianity appearance of the environment are the same, i.e., $d|\alpha_1(t)|/dt>0\Leftrightarrow d|\alpha_1(t)|^2/dt>0$. (ii) The monotonicity of $|\alpha_1(t)|^2$ and $|\alpha_1(t)|$ is the same. In this way, within a given actual evolution time, the effect of the parameters of the system and the environment on the BLP non-Markovianity $\mathcal{N}_{\rm BLP}$ of and the COMD non-Markovianity $\mathcal{N}_{\rm CMON}$ (i.e., see Figs. 6 and 7) are qualitatively the same for our model. Therefore, qualitatively, the relationship between BLP non-Markovianity and QSL also holds for CMON non-Markovianity. To be more clear, the QSL time is equal to the actual evolution time when $\mathcal{N}_{\rm CMON}=0$ (i.e., $\mathcal{N}_{\rm BLP}=0$), but the QSL time is smaller than the actual evolution time when $\mathcal{N}_{\rm CMON}>0$ (i.e., $\mathcal{N}_{\rm BLP}>0$). That is, the larger non-Markovianity $\mathcal{N}_{\rm CMON}$ can lead to the faster quantum evolution and the lower QSL time.

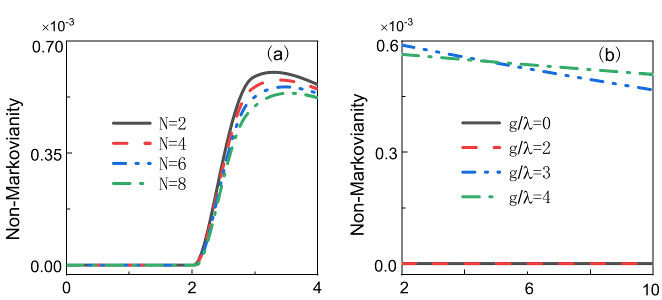

FIG. 6. (a), (b) The non-Markovianity $\mathcal{N}_{\rm CMON}$ of the quantum system dynamic with $\gamma_0=0.1\lambda$ and $\tau=1$ as a function of the coupling strength g/λ and the number of qubits N in the weak qubit-reservoir coupling regime.

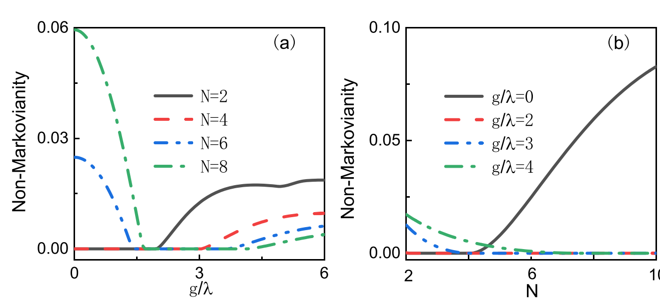

FIG. 7. (a), (b) The non-Markovianity $\mathcal{N}_{\rm CMON}$ of the quantum system dynamic with $\gamma_0=5\lambda$ and $\tau=1$ as a function of the coupling strength g/λ and the number of qubits N in the strong qubit-reservoir coupling regime.

APPENDIX C: TIGHTNESS OF QSL BOUND

In this Appendix, we provide some details for the bound tightness of the QSL in the models, complementing the conclusions shown in the text. To accurately evaluate the minimum time required for the system to evolve from the initial state ρ_0 to the target state ρ_τ, we should choose the QSL with good tightness and availability. According to Refs. [49,65], by measuring angles and distances between (mixed) states represented as generalized Bloch vectors, the authors derive quantum speed limits for arbitrary open quantum evolution, which can be Markovian or non-Markovian, providing fundamental bounds on the time required for the most general quantum dynamics. The QSL is given as follows:

$$\tau_{QSL} = \frac{\|\rho(0)-\rho(\tau)\|_{hs}}{\overline{\|\dot{\rho}(t)\|}}, \tag{C1}$$

where $(\overline{\|\dot{\rho}(t)\|}) = (1/\tau)\int_0^\tau dt\|\dot{\rho}(t)\|$ and $\|X\|_{hs} = \sum_i \sqrt{M_i^2}$. Here, M_i are the singular values of X. The authors also demonstrate that Eq. (B2) is easier to compute and measure than other QSL for open evolution, and that it is tighter than the previous bounds for almost all open processes.

For the dynamics evolution process we consider in this paper, $\|\rho(0)-\rho(\tau)\|_{hs} = \sqrt{2}(1-|\alpha_1(\tau)|^2)$, $\overline{\|\dot{\rho}(t)\|} = (1/\tau)\int_0^\tau dt\sqrt{2}\partial_t|\alpha_1(t)|^2$. QSL can be written as

$$\tau_{QSL} = \frac{1-|\alpha_1(\tau)|^2}{\frac{1}{\tau}\int_0^\tau |\partial_t|\alpha_1(t)|^2|dt}, \tag{C2}$$

. This is the same QSL bound proposed by Deffner *et al.* [33] that we choose in the paper [i.e., Eq. (7)]. Therefore, the bound tightness of the QSL chosen in this paper is good and can accurately evaluate the potential acceleration evolution ability of the system.

[1] H. P. Breuer and F. Petruccione, *Theory of Open Quantum Systems* (Oxford University Press, New York, 2002).

[2] M. A. Nielsen and I. L. Chuang, *Quantum Computation and Quantum Information* (Cambridge University Press, Cambridge, UK, 2000).

[3] I. de Vega and D. Alonso, Dynamics of non-Markovian open quantum systems, Rev. Mod. Phys. **89**, 015001 (2017).

[4] H.-P. Breuer, E.-M. Laine, J. Piilo, and B. Vacchini, *Colloquium:* Non-Markovian dynamics in open quantum systems, Rev. Mod. Phys. **88**, 021002 (2016).

[5] S. Cialdi, D. Brivio, E. Tesio, and M. G. A. Paris, Programmable entanglement oscillations in a non-Markovian channel, Phys. Rev. A **83**, 042308 (2011).

[6] A. Chiuri, C. Greganti, L. Mazzola, M. Paternostro, and P. Mataloni, Linear optics simulation of quantum non-Markovian dynamics, Sci. Rep. **2**, 968 (2012).

[7] B. H. Liu, L. Li, Y. F. Huang, C. F. Li, G. C. Guo, E. M. Laine, H. P. Breuer, and J. Piilo, Experimental control of the transition from Markovian to non-Markovian dynamics of open quantum systems, Nat. Phys. **7**, 931 (2011).

[8] C. F. Li, J. S. Tang, Y. L. Li, and G. C. Guo, Experimentally witnessing the initial correlation between an open quantum system and its environment, Phys. Rev. A **83**, 064102 (2011).

[9] J. Jin, V. Giovannetti, R. Fazio, F. Sciarrino, P. Mataloni, A. Crespi, and R. Osellame, All-optical non-Markovian stroboscopic quantum simulator, Phys. Rev. A **91**, 012122 (2015).

[10] S. Cialdi, M. A. C. Rossi, C. Benedetti, B. Vacchini, D. Tamascelli, S. Olivares, and M. G. A. Paris, All-optical quantum simulator of qubit noisy channels, Appl. Phys. Lett. **110**, 081107 (2017).

[11] B. Bellomo, R. L. Franco, and G. Compagno, Entanglement dynamics of two independent qubits in environments with and without memory, Phys. Rev. A **77**, 032342 (2008).

[12] Z. X. Man, Y. J. Xia, and R. Lo Franco, Harnessing non-Markovian quantum memory by environmental coupling, Phys. Rev. A **92**, 012315 (2015).

[13] J. S. Xu, K. Sun, C. F. Li, X. Y. Xu, G. C. Guo, E. Andersson, R. Lo Franco, and G. Compagno, Experimental recovery of quantum correlations in absence of system-environment back-action, Nat. Commun. **4**, 2851 (2013).

[14] B. M. Garraway, Nonperturbative decay of an atomic system in a cavity, Phys. Rev. A **55**, 2290 (1997).

[15] B. M. Garraway, Decay of an atom coupled strongly to a reservoir, Phys. Rev. A **55**, 4636 (1997).

[16] L. Mazzola, S. Maniscalco, J. Piilo, K.-A. Suominen, and B. M. Garraway, Pseudomodes as an effective description of memory: Non-Markovian dynamics of two-state systems in structured reservoirs, Phys. Rev. A **80**, 012104 (2009).

[17] E.-M. Laine, J. Piilo, and H.-P. Breuer, Witness for initial system-environment correlations in open-system dynamics, Europhys. Lett. **92**, 60010 (2010).

[18] J. Dajka, and J. Łuczka, Distance growth of quantum states due to initial system-environment correlations, Phys. Rev. A **82**, 012341 (2010).

[19] A. Smirne, H.-P. Breuer, J. Piilo, and B. Vacchini, Initial correlations in open-systems dynamics: The Jaynes-Cummings model, Phys. Rev. A **82**, 062114 (2010).

[20] A. Smirne, D. Brivio, S. Cialdi, B. Vacchini, and M. G. A. Paris, Experimental investigation of initial system-environment correlations via trace-distance evolution, Phys. Rev. A **84**, 032112 (2011).

[21] Z.-X. Man, A. Smirne, Y.-J. Xia, and B. Vacchini, Quantum interference induced by initial system–environment correlations, Phys. Lett. A **376**, 2477 (2012).

[22] H.-P. Breuer, E.-M. Laine, and J. Piilo, Measure for the degree of non-Markovian behavior of quantum processes in open systems, Phys. Rev. Lett. **103**, 210401 (2009).

[23] S. Lorenzo, F. Plastina, and M. Paternostro, Geometrical characterization of non-Markovianity, Phys. Rev. A **88**, 020102(R) (2013).

[24] A. Rivas, S. F. Huelga, and M. B. Plenio, Entanglement and non-Markovianity of quantum evolutions, Phys. Rev. Lett. **105**, 050403 (2010).

[25] E.-M. Laine, J. Piilo, and H.-P. Breuer, Measure for the non-Markovianity of quantum processes, Phys. Rev. A **81**, 062115 (2010).

[26] D. Chruściński, A. Kossakowski, and A. Rivas, Measures of non-Markovianity: Divisibility versus backflow of information, Phys. Rev. A **83**, 052128 (2011).

[27] D. Chruscinski and S. Maniscalco, Degree of non-Markovianity of quantum evolution, Phys. Rev. Lett. **112**, 120404 (2014).

[28] M. J. W. Hall, J. D. Cresser, L. Li, and E. Andersson, Canonical form of master equations and characterization of non-Markovianity, Phys. Rev. A **89**, 042120 (2014).

[29] B. Bellomo, R. Lo Franco, and G. Compagno, Non-Markovian effects on the dynamics of entanglement, Phys. Rev. Lett. **99**, 160502 (2007).

[30] S. F. Huelga, A. Rivas, and M. B. Plenio, Non-Markovianity-assisted steady state entanglement, Phys. Rev. Lett. **108**, 160402 (2012).

[31] A. W. Chin, S. F. Huelga, and M. B. Plenio, Quantum metrology in non-Markovian environments, Phys. Rev. Lett. **109**, 233601 (2012).

[32] Z.-X. Man, Y.-J. Xia, and R. Lo Franco, Cavity-based architecture to preserve quantum coherence and entanglement, Sci. Rep. **5**, 13843 (2015).

[33] S. Deffner and E. Lutz, Quantum speed limit for non-Markovian dynamics, Phys. Rev. Lett. **111**, 010402 (2013).

[34] Z. Sun, J. Liu, J. Ma, and X. Wang, Quantum speed limits in open systems: Non-Markovian dynamics without rotating-wave approximation, Sci. Rep. **5**, 8444 (2015).

[35] X. Meng, C. Wu, and H. Guo, Minimal evolution time and quantum speed limit of non-Markovian open systems, Sci. Rep. **5**, 16357 (2015).

[36] Y.-J. Zhang, W. Han, Y.-J. Xia, J.-P. Cao, and H. Fan, Quantum speed limit for arbitrary initial states, Sci. Rep. **4**, 4890 (2014).

[37] Y.-J. Zhang, W. Han, Y.-J. Xia, Y.-M. Yu, and H. Fan, Role of initial system-bath correlation on coherence trapping, Sci. Rep. **5**, 13359 (2015).

[38] A. D. Cimmarusti, Z. Yan, B. D. Patterson, L. P. Corcos, L. A. Orozco, and S. Deffner, Environment-assisted speed-up of the field evolution in cavity quantum electrodynamics, Phys. Rev. Lett. **114**, 233602 (2015).

[39] H.-B. Liu, W. L. Yang, J.-H. An, and Z.-Y. Xu, Mechanism for quantum speedup in open quantum systems, Phys. Rev. A **93**, 020105(R) (2016).

[40] Y.-J. Zhang, W. Han, Y.-J. Xia, J.-P. Cao, and H. Fan, Classical-driving-assisted quantum speed-up, Phys. Rev. A **91**, 032112 (2015).

[41] K. Xu, G.-F. Zhang, and W.-M. Liu, Quantum dynamical speedup in correlated noisy channels, Phys. Rev. A **100**, 052305 (2019).

[42] Z. Y. Xu and S. Q. Zhu, Quantum speed limit of a photon under non-Markovian dynamics, Chin. Phys. Lett. **31**, 020301 (2014).

[43] M. Cianciaruso, S. Maniscalco, and G. Adesso, Role of non-Markovianity and backflow of information in the speed of quantum evolution, Phys. Rev. A **96**, 012105 (2017).

[44] A. Goto, S. Ohki, K. Hashi, and T. Shimizu, Optical switching of nuclear spin–spin couplings in semiconductors, Nat. Commun. **2**, 378 (2011).

[45] M. O. Scully and M. S. Zubairy, *Quantum Optics* (Cambridge University Press, Cambridge, 1997).

[46] S. Ravets, H. Labuhn, D. Barredo, L. Béguin, T. Lahaye, A. Browaeys, Coherent dipole–dipole coupling between two single Rydberg atoms at an electrically-tuned Förster resonance, Nat. Phys. **10**, 914 (2014).

[47] M. Saffman, Quantum computing with atomic qubits and Rydberg interactions: Progress and challenges, J. Phys. B: At. Mol. Opt. Phys. **49**, 202001 (2016).

[48] I. Marvian and D. A. Lidar, Quantum speed limits for leakage and decoherence, Phys. Rev. Lett. **115**, 210402 (2015).

[49] F. Campaioli, F. A. Pollock, F. C. Binder, and K. Modi, Tightening quantum speed limits for almost all states, Phys. Rev. Lett. **120**, 060409 (2018).

[50] S. N. Sun, Y. G. Peng, X. H. Hu, and Y. J. Zheng, Quantum speed limit quantified by the changing rate of phase, Phys. Rev. Lett. **127**, 100404 (2021).

[51] G. Ness, A. Alberti, and Y. Sagi, Quantum speed limit for states with a bounded energy spectrum, Phys. Rev. Lett. **129**, 140403 (2022).

[52] S. N. Sun and Y. J. Zheng, Distinct bound of the quantum speed limit via the gauge invariant distance, Phys. Rev. Lett. **123**, 180403 (2019).

[53] N. B. An, J. Kim, K. Kim, Nonperturbative analysis of entanglement dynamics and control for three qubits in a common lossy cavity, Phys. Rev. A **82**, 032316 (2010).

[54] N. B. An, J. Kim, K. Kim, Entanglement dynamics of three interacting two-level atoms within a common structured environment, Phys. Rev. A **84**, 022329 (2011).

[55] S. Wißmann, A. Karlsson, E. M. Laine, J. Piilo, and H.-P. Breuer, Optimal state pairs for non-Markovian quantum dynamics, Phys. Rev. A **86**, 062108 (2012).

[56] Z. Y. Xu, S. Luo, W. L. Yang, C. Liu, and S. Q. Zhu, Quantum speedup in a memory environment, Phys. Rev. A **89**, 012307 (2014).

[57] J. Teittinen, H. Lyyra, and S. Maniscalco, There is no general connection between the quantum speed limit and non-Markovianity, New J. Phys. **21**, 123041 (2019).

[58] Y.-J. Zhang, X. Lu, H.-F. Lang, Z.-X. Man, Y.-J. Xia, and H. Fan, Quantum speedup dynamics process without non-Markovianity, Quantum. Inf. Process. **20**, 87 (2021).

[59] L. Krinner, M. Stewart, A. Pazmino, J. Kwon, and D. Schneble, Spontaneous emission of matter waves from a tunable open quantum system, Nature (London) **559**, 589 (2018).

[60] E. Vetsch, D. Reitz, G. Sagué, R. Schmidt, S. T. Dawkins, and A. Rauschenbeutel, Optical interface created by laser-cooled atoms trapped in the evanescent field surrounding an optical nanofiber, Phys. Rev. Lett. **104**, 203603 (2010).

[61] Y. Liu and A. A. Houck, Quantum electrodynamics near a photonic bandgap, Nat. Phys. **13**, 48 (2017).

[62] D. L. Underwood, W. E. Shanks, J. Koch, and A. A. Houck, Low-disorder microwave cavity lattices for quantum simulation with photons, Phys. Rev. A **86**, 023837 (2012).

[63] T. Chanda and S. Bhattacharya, Delineating incoherent non-Markovian dynamics using quantum coherence, Ann. Phys. **366**, 1 (2016).

[64] S. Maniscalco and F. Petruccione, Non-Markovian dynamics of a qubit, Phys. Rev. A **73**, 012111 (2006).

[65] F. Campaioli, F. A. Pollock, and K. Modi, Tight, robust, and feasible quantum speed limits for open dynamics, Quantum **3**, 168 (2019).